

Second harmonic hotspots at the edges of the unit cells in G-shaped gold nanostructures

Ventsislav K. Valev¹, Edward J. Osley^{2,3}, Ben De Clercq⁴, Alejandro V. Silhanek⁵, Paul A. Warburton^{2,3}, Oleg A. Aktsipetrov^{7,†}, Marcel Ameloot⁴, Victor V. Moshchalkov⁶ and Thierry Verbiest¹

¹ Molecular Electronics and Photonics, INPAC, KU Leuven, Celestijnenlaan 200 D, B-3001 Leuven, Belgium.

² London Centre for Nanotechnology, University College London, 17-19 Gordon Street, London, WC1H 0AH, United Kingdom

³ Department of Electronic and Electrical Engineering, University College London, Torrington Place, London, WC1E 7JE, United Kingdom

⁴ University Hasselt and transnational University Limburg, BIOMED, Agoralaan building C, B-3590, Diepenbeek, Belgium

⁵ Département de Physique, Université de Liège, Bât. B5, Allée du 6 août, 17, Sart Tilman, B-4000 (Belgium)

⁶ Nanoscale Superconductivity and Magnetism, Pulsed Fields Group, INPAC, KU Leuven, Celestijnenlaan 200 D, B-3001 Leuven, Belgium.

*Corresponding author: v.k.valev@fys.kuleuven.be

ABSTRACT

We report our latest results on second harmonic generation (SHG) microscopy from arrays of G-shaped chiral gold nanostructures. The nanostructures are arranged in unit cells composed of four Gs, each rotated at 90° with respect to its neighbors. As it has already been demonstrated, for linearly polarized light, these unit cells yield a pattern of four SHG hotspots. However, upon increasing the pitch of the nanostructured arrays, extra hotspots can be observed at the edges of the unit cells. While the origin of these extra hotspots remains to be elucidated, their position indicates a relationship to coupling behavior between the unit cells.

Keywords: Second Harmonic Generation, SHG, metamaterials, nanostructures, chirality, nanoscience, nonlinear optics, plasmonics

INTRODUCTION

The term "electromagnetic hotspots" designates regions where the electromagnetic energy is highly concentrated. These hotspots have attracted a lot of attention because they can lead to extreme enlargement of molecular optical response.^{1,2} A striking example is surface enhanced Raman scattering,³ whereby the Raman signal can be increased fourteen orders of magnitude.^{4,5} The hotspots themselves can originate in the electromagnetic lightning rod effect or in plasmonic local field enhancements. The latter constitute essentially a collective excitation of the conduction band electrons at a sample surface. The canonical example of surface plasmon excitation is the small (with respect to the wavelength) spherical gold nanoparticle, whereby the electron cloud can oscillate in response to the electric field of light. While a single gold nanoparticle is conceptually very appealing to illustrate surface plasmon field enhancements, in the experimental studies of more complex systems, these field enhancements are often difficult to separate

[†] Regretfully, Prof. Oleg A. Aktsipetrov passed away in the autumn of 2011.

from other optical phenomena, such as scattering, diffraction or antenna effects. However, recently, it has been demonstrated that second harmonic generation (SHG) provides the means for effectively mapping plasmonic hotspots while effectively filtering the unwanted signal.

SHG refers to the processes whereby two photons at the frequency of illumination are converted into a single photon at the double frequency. This process is universal in the sense that it occurs through virtual energy levels, at any frequency of light, and does not require the presence of a particular resonance. Surface SHG is a nonlinear optical process that requires the use of high intensity incident light sources, such as ultrafast laser systems. High intensity can also be achieved within electromagnetic hotspots and, as a consequence, second harmonic imaging of such hotspots is obtained. Because the detected light is at the second harmonic of the incident light, all the linear optical "noise" is effectively filtered from the signal.

Within the dipole approximation, the SHG process is forbidden in centrosymmetric systems. Symmetry is broken at the surfaces and interfaces of materials, which allows SHG to be surface/interface-sensitive down to the atomic monolayer.⁶ Symmetry is also broken by externally applied electric⁷ or magnetic⁸ dc fields, though, in the case of the latter, care should be taken in interpreting the results.⁹ These breaks in symmetry allow SHG to successfully image ferroelectric¹⁰ and ferromagnetic¹¹ domains. Let us consider again a small gold nanoparticle. Gold has a face centered cubic crystal structure, which means that it is centrosymmetric. Moreover, the overall spherical shape is also centrosymmetric. It follows that, in the absence of externally applied electric or magnetic fields, the canonical example for plasmon local field enhancements should not give rise to any second harmonic signal. However, experimentally it has been demonstrated that surface plasmon resonances do give rise to an enhanced second harmonic signal.¹² In this work, the authors have tuned the frequency of plasmon resonance in gold core silver shell nanoparticles, by varying the proportions of both metals. Additionally, strong second harmonic signal was observed from 4 nm large gold clusters,¹³ from gold colloids with sizes ranging from 5-22 nm,¹⁴ from gold nanoparticles with 11 nm diameter¹⁵ and from silver nanoparticles with diameter of 40 nm.¹⁶ Interestingly, in the latter work, polarization measurements demonstrated that, although forbidden in the dipole approximation, the second harmonic signal is of dipolar origin.

The "forbidden" signal was attributed to small deviations in shape from the centrosymmetry of the nanoparticles, since in clearly noncentrosymmetric nanoparticles, such as nanorods¹⁷ or decahedra,¹⁸ the SHG signal is allowed. In fact, the latter investigation goes further and compares the SHG signal with that of spherical nanoparticles as a function of size, within the range 17 to 150 nm. The authors show that above 50 nm, the SHG signal from spherical and decahedral nanostructures is comparable, which indicates a common origin - multipolar contributions and retardation effects. However, below that size, the difference in centrosymmetry plays an important role. The idea that different SHG mechanisms are at work depending on the size of plasmonic nanoparticles has also been experimentally confirmed upon studying gold nanoparticles within the range 10 to 150 nm^{19,20} and silver nanoparticles within the range 20 to 80 nm,²¹ a theoretical model, based on phenomenological parameters has also been proposed to account for this size dependence.²² To summarize: for smaller nanoparticles the SHG signal is of dipolar origin and it originates at the (non perfectly spherical) surface of the nanoparticles, where plasmon field enhancements also occur, while for larger nanoparticles, the SHG signal contains multipolar terms and has been attributed to retardation effects. We can already say that a similar behavior is encountered for continuous thin films made of centrosymmetric materials. Indeed, in such systems, a dipolar SHG signal is associated with the monolayer thick surfaces and interfaces, while a multipolar SHG signal is associated with the bulk of the films. However, before we speak about thin films, let us briefly address the sensitivity of SHG to plasmonic field enhancements as complexity builds up from single nanoparticles.

When two plasmonic nanoparticles are placed in close proximity, plasmonic coupling takes place and can lead to SHG enhancements. Such enhancements were reported upon numerically simulating two silver nanorods separated by 28 nm²³ and two gold nanorods separated by 30 nm.²⁴ Moreover, it was theoretically shown that, in coupled plasmonic nanostructures, the overall SHG is related to the electromagnetic energy per unit length stored in the gap area between the nanostructures.²⁵ Experimental work on nanowires has also demonstrated enhanced SHG due to plasmonic coupling between nanostructures.^{26,27} In particular, it has been shown that, upon aggregating gold nanoparticles by means of molecular binding, the second harmonic signal is significantly enlarged.²⁸ While such an assembly of nanoparticles is random, more

ordered configuration have also been studied, such as nanocylinders.²⁹ Besides direct coupling and possible retardation effects, an ordered chain of nanoparticles can support propagating plasmons, a phenomenon that has also been followed by SHG.^{30,31} An alternative geometry for studying the interaction of propagating plasmons with nanoparticles consists in using continuous films as support for the propagating plasmons and employing the nanoparticles as scatters.³² Strong local field enhancements are also present at rough surfaces of continuous films, and in these systems too SHG proves to be a successful probe.³³ The reason for this success is that surface roughness can be regarded as an abundance of symmetry-breaking defects which are localized at the sample surface and such defects are well known sources of SHG.^{34,35} As complexity builds up from single particles to ordered arrays, second harmonic imaging microscopy offers an effective way to map the plasmonic hotspots.^{36,37,38}

While SHG microscopy can be employed for detecting single nanoparticles,^{39,40} where the hotspots coincide with the position of the nanostructures, the technique is particularly interesting in the case of ordered arrays, where the pattern of hotspots can differ significantly from that of the underlying nanogeometry.^{41,42} In this manner it is possible to experimentally determine in which part of the nanostructures are the hotspots originating.⁴³ Although visualization is limited by the resolution limit, we have recently demonstrated that, for sufficiently high incoming light intensity, the hotspots can be imprinted onto the surface of the nanostructures themselves through nanobump and nanojet formation, for subsequent imaging with surface probe techniques.^{44,45}

Here we report our recent results on studying a nanostructured sample array, composed of G-shaped gold nanostructures. We find that upon increasing pitch of the array, more SHG hotspots appear. While the precise origin of these hotspots remains to be determined, their position on the edges of the unit cell seems to indicate a relation to coupling effects between unit cells.

SAMPLE PREPARATION AND EXPERIMENTS

The samples consists of G-shaped gold nanostructures arranged according to the pattern in Fig. 1a. During fabrication, a Si substrate covered with a thermally grown layer of silicon dioxide approximately 100 nm

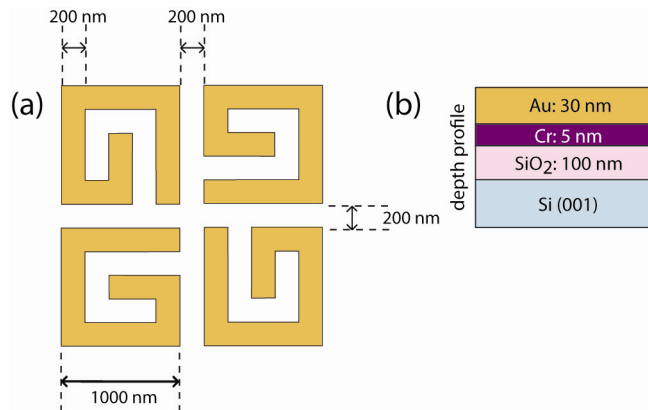


Fig.1. In (a), schematic diagram G-shaped gold nanostructures arranged in a unit cell for the nanostructured sample array. The dimensions correspond to the first sample at study, having a pitch of 2.3 μm . In (b), the depth profile for the nanostructures is shown.

thick was coated with a solution of poly(methyl methacrylate) (PMMA) dissolved in Anisole. The substrate was then spun at 2000 RPM for 45 seconds and then heated on a hotplate at 150 Celsius for 75 seconds producing a 100 nm thick layer of PMMA resist. The PMMA layer was then patterned using electron beam lithography (EBL) and the exposed areas of PMMA resist removed using a developer consisting of 1 part 4-Methyl-2-pentanone (MIBK) to 3 parts Isopropyl alcohol (IPA). The EBL masked sample was then placed in a thermal evaporation chamber which was evacuated to a base pressure below 1×10^{-6} mBar. A 5

nm chromium adhesion layer was evaporated onto the sample using a resistively heated tungsten wire basket, followed by a 30 nm gold layer deposited from a resistively heated *molybdenum* boat. The coated sample was then placed in an acetone bath for several hours, sonication of the bath then removed the unexposed PMMA and its metallic coating leaving behind the metal features. The depth profile of the samples following this fabrication procedure is shown in Fig. 1b. Further details on fabrication can be found in Ref. [46].

In order to study the possible coupling between nanostructures, three samples of nanostructured arrays were prepared with increasing pitch. More specifically, the pitch was set at 2.3 μm , 2.5 μm and 2.6 μm ; scanning electron microscopy pictures of the corresponding sample arrays can be seen in Fig. 2a, 2b and 2c, respectively. Please note that, due to a slight difference in EBL dosage, the size of the nanostructures in Fig. 2a differs from the others. This difference could have important consequences and has been taken into account when interpreting the SHG results.

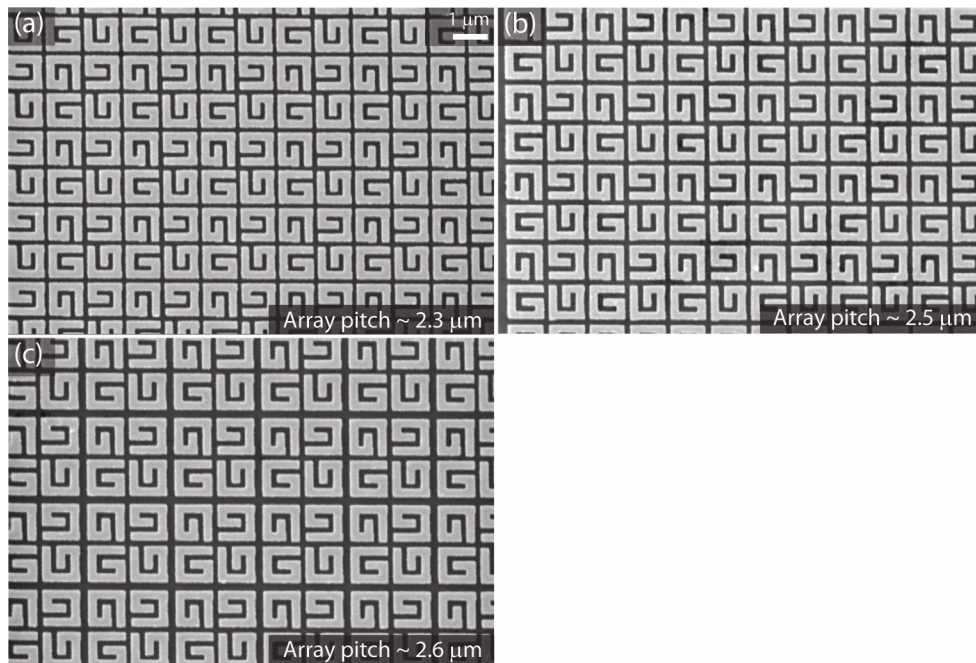


Fig.2. Scanning electron microscopy images of the sample arrays. In (a), the pitch of the array is set at 2.3 μm . In (b), the pitch of the array is set at 2.5 μm . In (c), the pitch of the array is set 2.6 μm .

Second harmonic generation microscopy is performed by adapting a Zeiss LSM 510 Laser Scanning Microscope (Carl Zeiss, Jena, Germany). During measurements the laser spot is scanned at adjustable speed and direction over the sample surface. The illumination itself is performed by means of a pulsed Ti:Sapphire laser (Mai Tai, Newport-Spectra Physics), with 800 nm wavelength. The laser pulses are at a frequency of 80.1 MHz and they are dispersion corrected by a Deep See module following the laser. The SHG-signal is separated from the incident light by a dichroic mirror (HFT KP650) and additional shortpass filter (KP660). Images were made with a 100x objective with numerical aperture of 1.46, the spot size on the sample is approximately 400 nm in diameter. Further details regarding the microscope configuration and procedure can be found in Ref. [47].

RESULTS

Figure 3a shows the SHG hotspot pattern that is obtained, for linearly polarized light along the horizontal direction, from the nanostructured sample array with 2.3 μm pitch. The hotspots are indicated by purple

spots on the black background of the substrate. The unit cell response consists of four hotspots oriented along the main diagonal of the square unit cell; due to their proximity, the middle two hotspots are somewhat difficult to resolve. Almost no off diagonal hotspots can be seen in Fig. 3a. At variance, in Fig. 3b, which corresponds to the nanostructured sample array with 2.5 μm pitch, besides the four hotspots along the main diagonal, there are two off diagonal hotspots. The color coded intensity in this picture increases following the rainbow color order. High intensity spots are due to a combination of laser-induced damage on the sample and fabrication defects. It should be noted that in Fig. 3b, each individual unit cell is clearly distinguishable from its neighbors – the hotspot patterns of the unit cells are separated by clear black lines. Interestingly, upon increasing the pitch of the sample arrays from 2.5 μm to 2.6 μm , this distinction disappears. More specifically, in Fig. 3c, the hotspot pattern of the unit cell is composed of four hotspots along the main diagonal as in Fig. 3a, plus two off diagonal hotspots as in Fig. 3b, plus six hotspots at the exterior edges of the unit cells that are oriented along the direction of polarized light.

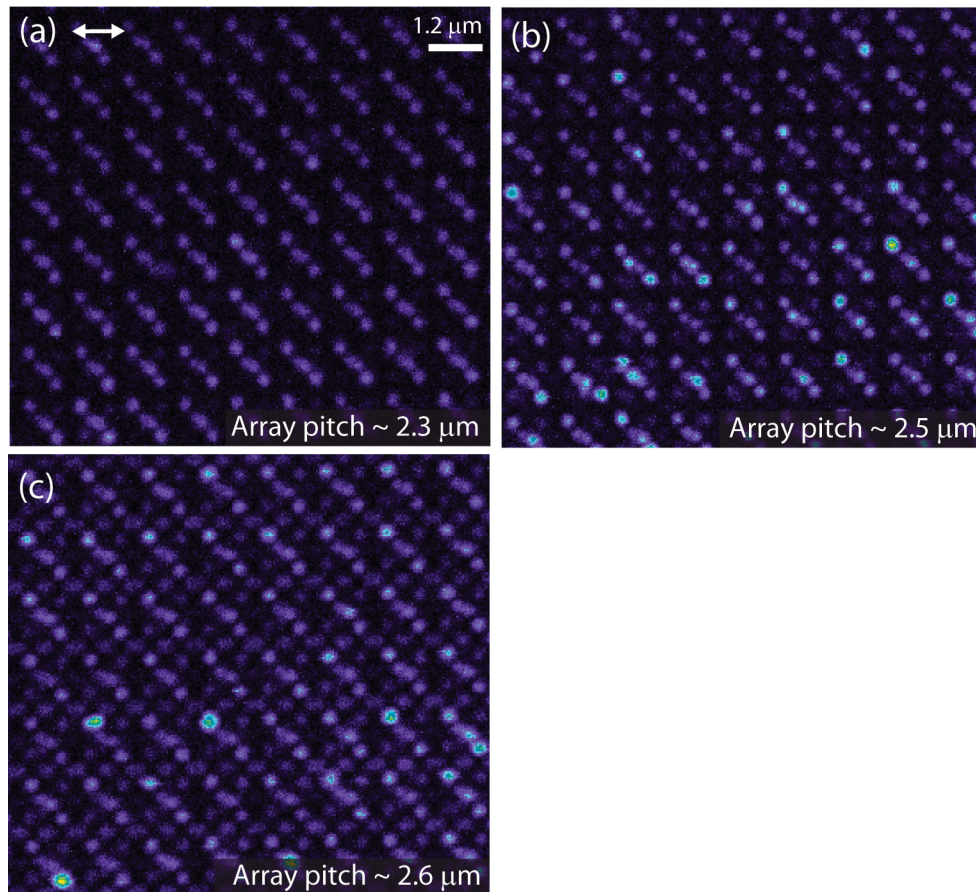


Fig.3. Second Harmonic Generation (SHG) microscopy of the sample arrays at study. In (a), for an array with 2.3 μm pitch, four hotspots along the main diagonal of the unit cell can be observed. In (b), for an array with 2.5 μm pitch, two off diagonal hotspots appear. In (c), for an array with 2.6 μm pitch, additional hotspots can be seen. The color-coded intensities increase from black, through purple, to blue.

OUTLOOK

We have applied second harmonic generation microscopy to the study of G-shaped, gold nanostructures. This technique is showing increasing potential for mapping plasmonic hotspots in nanostructured arrays. Figure 3 shows a very clear trend in the experimental results – with increasing pitch of the sample arrays,

more hotspots become apparent. Although very promising these results are preliminary. More careful investigation of the increase in pitch will be undertaken by producing novel sample series covering a large range of pitch variation. Reproducibility of the results will also be checked against variation of the EBL dosage. The precise position of the extra hotspots will be determined by imprinting them on the sample surface, using plasmons-assisted sub-wavelength laser-ablation. The precise origin of these hotspots will be investigated with rigorous numerical simulations.

ACKNOWLEDGEMENTS

We acknowledge financial support from the Fund for scientific research Flanders (FWO-V), the University of Leuven (GOA, CREA), Methusalem Funding by the Flemish government and the Belgian Inter-University Attraction Poles IAP Programmes. V.K.V. is grateful for the support from the FWO-Vlaanderen. O.A.A. was partly supported by the Russian Foundation for Basic Research.

REFERENCES

-
- [1] Jeanmaire, D.L. and Van Duyne, R.P., "Surface raman spectroelectrochemistry: Part I. Heterocyclic, aromatic and aliphatic amines adsorbed on the anodized silver electrodes," *J. Electroanal. Chem.* 84, 1–20 (1977).
- [2] Albrecht, M.G. and Creighton, J.A., "Anomalously intense Raman spectra of pyridine at a silver electrode," *J. Am. Chem. Soc.* 99, 5215–5217 (1977).
- [3] Stockman, M. I., "Surface-Enhanced Raman Scattering: Physics and Applications," *Top. Appl. Phys.* 103, 47 (2006).
- [4] Kneipp, K., Wang, Y., Kneipp, H., Perelman, L. T., Itzkan, I., Dasari, R. R. and Feld, M. S., "Single molecule detection using surface-enhanced raman scattering (sers)," *Phys. Rev. Lett.* 78, 1667 (1997).
- [5] Nie, S. and Emory, S. R., "Probing single molecules and single nanoparticles by surface-enhanced Raman scattering," *Science* 275, 1102 (1997).
- [6] Valev, V. K., Kirilyuk, A., Rasing, Th., Dela Longa, F., Kohlhepp, J. T. and Koopmans, B., "Oscillations of the net magnetic moment and magnetization reversal properties of the Mn/Co interface," *Phys. Rev. B* 75, 012401 (2007).
- [7] Lee, C. H., Chang, R. K. and Bloembergen, N., "Nonlinear electroreflectance in silicon and silver," *Phys. Rev. Lett.* 18(5), 167–170 (1967).
- [8] Kirilyuk, A. and Rasing, Th., "Magnetization-induced-second-harmonic generation from surfaces and interfaces," *J. Opt. Soc. Am. B* 22(1), 148–167 (2005).
- [9] Valev, V. K., Gruyters, M., Kirilyuk, A. and Rasing, Th., "Influence of quadratic contributions in magnetization-induced second harmonic generation studies of magnetization reversal," *Phys. Stat. Sol. (b)* 242, 3027–3031 (2005).
- [10] Sheng, Y., Best, A., Butt, H.-J., Krolkowski, W., Arie, A. and Koynov, K., "Three-dimensional ferroelectric domain visualization by Cerenkov-type second harmonic generation," *Opt. Express* 18(16), 16539–16545 (2010).
- [11] Pavlov, V. V., Ferré, J., Meyer, P., Tessier, G., Georges, P., Brun, A., Beauvillain, P. and Mathet, V., "Linear and non-linear magneto-optical studies of Pt/Co/Pt thin films," *J. Phys. Condens. Matter* 13(44), 9867–9878 (2001).
- [12] Abid, J.P., Nappa, J., Girault, H.H. and Brevet, P.F. "Pure Surface Plasmon Resonance Enhancement of the First Hyperpolarizability of Gold Core – Silver Shell Nanoparticles," *J. Chem. Phys.*, 121, 12577 (2004).
- [13] Antoine, R., Péllarin, M., Prével, B., Palpant, B., Broyer, M., Galletto, P., Brevet, P.F. and Girault, H.H., "Surface Plasmon Enhanced Second Harmonic Response from Gold Clusters Embedded in an Alumina Matrix," *J. Appl. Phys.*, 84, 4532 (1998).
- [14] Galletto, P., Brevet, P.F., Girault, H.H., Antoine, R. and Broyer, M., "Size Dependence of the Surface Plasmon Enhanced Second Harmonic Response of Gold Colloids: Towards a New Calibration Method," *Chem. Commun.* 7, 581-582 (1999).
- [15] Russier-Antoine, I., Nappa, J., Benichou, E., Jonin, Ch. and Brevet, P.F., "Wavelength Dependence of the Hyper Rayleigh Scattering Response from Gold Nanoparticles" *J. Chem. Phys.* 120, 10748 (2004).
- [16] Nappa, J., Russier-Antoine, I., Benichou, E., Jonin, Ch. and Brevet, P.F., "Wavelength Dependence of the Retardation Effects in Silver Nanoparticles Followed by Polarization Resolved Hyper Rayleigh Scattering," *Chem. Phys. Lett.*, 415, 246 (2005).
- [17] Nappa, J., Revillod, G., Abid, J.P., Russier-Antoine, I., Jonin, Ch., Benichou, E., Girault, H.H. and Brevet, P.F., "Hyper Rayleigh Scattering of Gold Nanorods and their relationship with linear assemblies of gold nanospheres," *Faraday Disc.*, 125, 145 (2004).

- [18] Russier-Antoine, I., Duboisset, J., Bachelier, G., Benichou, E., Jonin, Ch., Del Fatti, N., Vallée, F., Sanchez-Iglesias, A., Pastoriza-Santos, I., Liz-Marzan, L.M. and Brevet, P.F. "Symmetry Cancellations in the Quadratic Hyperpolarizability of Non Centrosymmetric Gold Decahedra," *J. Phys. Chem. Lett.*, 1, 874 (2010).
- [19] Nappa, J., Revillod, G., Russier-Antoine, I., Benichou, E., Jonin, Ch. and Brevet, P.F., "Electric Dipole Origin of the Second Harmonic Generation from Small Metallic Particles," *Phys. Rev. B* 71, 165407 (2005).
- [20] Nappa, J., Russier-Antoine, I., Benichou, E., Jonin, Ch. and Brevet, P. F., "Second-harmonic light generation from small gold metallic particles: From the dipolar to the quadrupolar response," *J. Chem. Phys.* 125, 184712 (2006).
- [21] Russier-Antoine, I., Benichou, E., Bachelier, G., Jonin, Ch. and Brevet, P.F., "Multipolar Contributions of the Second Harmonic Generation from Silver and Gold Nanoparticles," *J. Phys. Chem. C*, 111, 9044 (2007).
- [22] Bachelier, G., Russier-Antoine, I., Benichou, E., Jonin, Ch. and Brevet, P.F., "Multipolar Second Harmonic Generation in Noble Metal Nanoparticles," *J. Opt. Soc. Am. B*, 25, 955 (2008).
- [23] Centini, M., Benedetti, A., Sibilia, C. and Bertolotti, M., "Coupled 2D Ag nano-resonator chains for enhanced and spatially tailored second harmonic generation," *Opt. Express* 19, 8218-8232 (2011).
- [24] Benedetti, A., Centini, M., Bertolotti, M. and Sibilia, C. "Second harmonic generation from 3D nanoantennas: on the surface and bulk contributions by far-field pattern analysis," *Opt. Express* 19, 26752 (2011).
- [25] Benedetti, A., Centini, M., Sibilia, C. and Bertolotti, M., "Engineering the second harmonic generation pattern from coupled gold nanowires," *J. Opt. Soc. Am. B* 27(3), 408–416 (2010).
- [26] Belardini, A., Larciprete, M. C., Centini, M., Fazio, E., Sibilia, C., Bertolotti, M., Toma, A., Chiappe, D. and Buatier de Mongeot, F., "Tailored second harmonic generation from self-organized metal nano-wires arrays," *Opt. Express* 17(5), 3603–3609 (2009).
- [27] Belardini, A., Larciprete, M. C., Centini, M., Fazio, E., Sibilia, C., Chiappe, D. Martella, C., Toma, A., Giordano, M. and Buatier de Mongeot, F., "Circular Dichroism in the Optical Second-Harmonic Emission of Curved Gold Metal Nanowires," *Phys. Rev. Lett.* 107, 257401 (2011).
- [28] Russier-Antoine, I., Huang, J., Benichou, E., Bachelier, G., Jonin, Ch. and Brevet, P.F., "Hyper Rayleigh Scattering of Protein-Mediated Gold Nanoparticles Aggregates," *Chem. Phys. Lett.*, 450, 345 (2008).
- [29] Awada, Ch., Kessi, F., Jonin, Ch., Adam, P.M., Kostcheev, S., Bachelot, R., Royer, P., Russier-Antoine, I., Benichou, E., Bachelier, G. and Brevet, P.F., "On- and Off-Axis Second Harmonic Generation from an Array of Gold Metallic Nanocylinders," *J. Appl. Phys.* 110, 023109 (2011).
- [30] Biris, C.G. and Panoiu, N. C., "Excitation of dark plasmonic cavity modes via nonlinearly induced dipoles: applications to near-infrared plasmonic sensing," *Nanotechnology* 22, 235502 (2011).
- [31] Biris, C. G. and Panoiu, N. C. "Excitation of linear and nonlinear cavity modes upon interaction of femtosecond pulses with arrays of metallic nanowires," *Appl Phys A* 103, 863–867 (2011).
- [32] Cao, L., Panoiu, N. C. and Osgood, R. M., "Surface second-harmonic generation from surface plasmon waves scattered by metallic nanostructures," *Phys. Rev. B* 75, 205401 (2007).
- [33] Smolyaninov, I.I., Zayats, A.V. and Davis, C.C., "Near-field second harmonic generation from a rough metal surface," *Phys. Rev. B* 56, 9290–9293 (1997).
- [34] Zayats, A.V., Kalkbrenner, T., Sandoghdar, V. and Mlynek, J., "Second-harmonic generation from individual surface defects under local excitation," *Phys. Rev. B* 61, 4545 (2000).
- [35] Canfield, B.K., Kujala, S., Laiho, K., Jefimovs, K., Turunen, J. and Kauranen, M., "Chirality arising from small defects in gold nanoparticle arrays," *Opt. Express* 14, 950-955 (2006).
- [36] Zayats, A.V., Smolyaninov, I.I. and Davis, C.C., "Observation of localized plasmonic excitations in thin metal films with near-field second-harmonic microscopy," *Opt. Commun.* 169, 93–96 (1999).
- [37] Anceau, C., Brasselet, S., Zyss, J. and Gadenne, P., "Local second-harmonic generation enhancement on gold nanostructures probed by two-photon microscopy," *Opt. Lett.* 28, 713–715 (2003).
- [38] Valev, V. K., Silhanek, A. V., Smisdom, N., De Clercq, B., Gillijns, W., Aktsipetrov, O. A., Ameloot, M., Moshchalkov, V. V. and Verbiest, T., "Linearly Polarized Second Harmonic Generation Microscopy Reveals Chirality," *Optics Express*, 18, 8286-8293 (2010).
- [39] Butet, J., Duboisset, J., Bachelier, G., Russier-Antoine, I., Benichou, E., Jonin, C. and Brevet, P.-F. "Optical Second Harmonic Generation of Single Metallic Nanoparticles Embedded in a Homogeneous Medium," *Nano Lett.* 10, 1717–1721 (2010).
- [40] Butet, J., Bachelier, G., Duboisset, J., Bertorelle, F., Russier-Antoine, I., Jonin, C., Benichou, E. and Brevet, P.-F., "Three-dimensional mapping of single gold nanoparticles embedded in a homogeneous transparent matrix using optical second-harmonic generation," *Opt. Express* 18, 22314–22323 (2010).
- [41] Valev, V. K., Smisdom, N., Silhanek, A. V., De Clercq, B., Gillijns, W., Ameloot, M., Moshchalkov, V. V. and Verbiest, T. "Plasmonic Ratchet Wheels: Switching Circular Dichroism by Arranging Chiral Nanostructures," *Nano Lett.* 9, 3945 (2009).
- [42] Valev, V. K., Volodin, A., Silhanek, A. V., Gillijns, W., De Clercq, B., Jeyaram, Y., Paddubrouskaya, H., Biris, C. G., Panoiu, N. C., Aktsipetrov, O. A., Ameloot, M., Moshchalkov, V. V. and Verbiest, T., "Plasmons reveal the direction of magnetization in nickel nanostructures," *ACS Nano*, 5, 91-96 (2011).

- [43] Valev, V. K., Silhanek, A. V., De Clercq, B., Gillijns, W., Jeyaram, Y., Zheng, X., Volskiy, V., Aktsipetrov, O. A., Vandenbosch, G. A. E., Ameloot, M., Moshchalkov, V. V. and Verbiest, T., "U-shaped switches for optical information processing at the nanoscale," *Small* 7, 2573-2576 (2011).
- [44] Valev, V. K., Silhanek, A. V., Jeyaram, Y., Denkova, D., De Clercq, B., Petkov, V., Zheng, X., Volskiy, V., Gillijns, W., Vandenbosch, G. A. E., Aktsipetrov, O. A., Ameloot, M., Moshchalkov, V. V. and Verbiest, T., "Hotspot decorations map plasmonic patterns with the resolution of scanning probe techniques," *Phys. Rev. Lett.* 106, 226803 (2011).
- [45] Valev, V. K., Denkova, D., Zheng, X., Kuznetsov, A. I., Reinhardt, C., Chichkov, B. N., Tsutsumanova, G., Osley, E.J., Petkov, V., De Clercq, B., Silhanek, A. V., Jeyaram, Y., Volskiy, V., Warburton, P. A., Vandenbosch, G. A. E., Russev, S., Aktsipetrov, O. A., Ameloot, M., Moshchalkov, V. V. and Verbiest, T., "Plasmon-enhanced sub-wavelength laser ablation: plasmonic nanojets," *Adv. Mater.* 24, OP29-OP35 (2012).
- [46] Valev, V. K., Zheng, X., Biris, C.G., Silhanek, A.V., Volskiy, V., De Clercq, B., Aktsipetrov, O.A., Ameloot, M., Panoiu, N.C., Vandenbosch, G. A. E. and Moshchalkov, V. V., "The Origin of Second Harmonic Generation Hotspots in Chiral Optical Metamaterials," *Opt. Mater. Express* 1, 36-45 (2011).
- [47] Valev, V. K., De Clercq, B., Zheng, X., Denkova, D., Osley, E. J., Vandendriessche, S., Silhanek, A. V., Volskiy, V., Warburton, P. A., Vandenbosch, G. A. E., Ameloot, M., Moshchalkov, V. V. and Verbiest, T., "The role of chiral local field enhancements below the resolution limit of Second Harmonic Generation microscopy," *Opt. Express* 20, 256-264 (2012).